15th Australasian Fluid Mechanics Conference
The University of Sydney, Sydney, Australia
13-17 December 2004

Modelling Gas-Liquid Bubbly Flows

G.H. Yeoh[1] and J. Y. Tu[2]

[1]Australian Nuclear Science and Technology Organisation (ANSTO)
PMB 1, Menai, NSW, 2234 AUSTRALIA

[2]School of Aerospace, Mechanical and Manufacturing Engineering
RMIT University, Victoria, 3083 AUSTRALIA

Abstract

In this paper, modelling gas-liquid bubbly flows is achieved by the introduction of a population balance equation combined with the three-dimensional two-fluid model. An average bubble number density transport equation has been incorporated in the commercial code CFX5.7 to better describe the temporal and spatial evolution of the geometrical structure of the gas bubbles. The coalescence and breakage effects of the gas bubbles are modelled according to the coalescence by the random collisions driven by turbulence and wake entrainment while for bubble breakage by the impact of turbulent eddies. Local radial distributions of the void fraction, interfacial area concentration, bubble Sauter mean diameter, and gas and liquid velocities, are compared against experimental data obtained at Prudue University. Satisfactory agreements for the local distributions are achieved between the predictions and measurements.

Introduction

The range of applications for two-phase flow systems is immense. In many chemical industries, bubble column reactors are extensively employed for handling processes that require large interfacial area and efficient mixing processes. Engineering systems such as heat exchangers also widely employ the two-phase flow mixture of gas and liquid for efficient removal of heat generation. In the nuclear area, the capability to predict void fraction profile and other two-phase flow parameters in subcooled boiling flows is of considerable importance to ensure the safe operation of the reactor.

In the present state-of-the-art, the two-fluid model can be considered as the most detailed and accurate macroscopic formulation of the thermal-hydraulic dynamics of two-phase flow systems. Within the field equations, expressed by conservation of mass, momentum and energy for each phase, interfacial transfer terms appear in each of the equations. These terms determine the rate of phase changes and the degree of mechanical and thermal non-equilibrium between phases. They represent essential closure relations, which should be modelled accurately. However, the closure relations for the interfacial transfer terms are presently far from resolution and they are still the weakest link in the two-fluid model.

In the two-fluid model, the interfacial transfer terms are strongly related to the interfacial area concentration and the local transfer mechanisms such as the degree of turbulence near the interfaces. Fundamentally, the interfacial transport of mass, momentum and energy is proportional to the interfacial area concentration a_{if} and driving forces. The interfacial area concentration (interfacial area per unit volume) characterises the kinematic effects; it is related to the geometrical effects of the interfacial structure. Nevertheless, the driving forces for the inter-phase transport characterises the local transport mechanism.

Since the interfacial area concentration a_{if} represents the key parameter that links the interaction of the phases, much attention have been concentrated towards better understanding the coalescence and breakage effects due to interactions among bubbles and between bubbles and turbulent eddies for gas-liquid bubbly flows. The primary aim is to better describe the temporal and spatial evolution of the two-phase geometrical structure. Some empirical correlations [1], models [2], population balance approaches [3], volumetric interfacial area transport equation [4-6] have been proposed to predict the interfacial area concentration.

The MUSIG (Multiple Size Group) model has been implemented in CFX4.4 to account for the non-uniform bubble size distribution in a gas-liquid mixture. In CFX5.7, it is currently provided as a beta version. The model was developed by Lo [7] and solves a range of bubble classes. Because of the possible wide range of bubble sizes that may exist in the two-phase flow system, it requires a substantial number of equations to adequately track the bubble sizes. From our recent studies [8] of a subcooled boiling flow in an annulus channel, we have employed 15 transport equations in addition to the two sets of conservation equations of mass, momentum and energy to track the range of bubbles sizes ranging from 0 mm to 9.5 mm in diameter. For flows where large bubbles can exist especially in bubble column reactors, this could amount to the consideration of greater than 15 transport equations, which the numerical effort to solve such problem could be enormous. Therefore in practical calculations if the bubble classes chosen are limited, the size distribution of the bubbles cannot be adequately represented.

In this paper, the average number density transport equation is considered. Here, only one additional equation is solved. To demonstrate the possibility of a simpler approach of combining population balance with computational fluid dynamics (CFD), this transport equation is implemented in the generic commercial CFD code CFX5.7. In this equation, the coalescence and breakage mechanisms of the bubble are accommodated for the gas phase. The two-fluid and standard k-ε models are employed. Within the source terms of the turbulent kinetic energy k, the energy exchange between the interfacial free energy and liquid turbulent kinetic energy due to bubble coalescence and breakage is incorporated. Respective coalescence and breakage mechanisms by Wu et al. [4], Hibiki and Ishii [5] and Yao and Morel [6], implemented as source terms in the average number density transport equation, are assessed. The model predictions are compared against experimental data of an isothermal gas-liquid bubbly flow in a vertical pipe performed in Prudue University [5].

Physical Model

Governing Equations

The numerical simulations presented are based on the two-fluid model Eulerian-Eulerian approach. The Eulerian modelling framework is based on ensemble-averaged mass and momentum

transport equations for each phase. Regarding the liquid phase (α_l) as continuum and the gaseous phase (bubbles) as disperse phase (α_g), these equations without mass transfer can be written as:

$$\frac{\partial \rho_k \alpha_k}{\partial t} + \nabla \cdot \left(\rho_k \alpha_k \vec{u}_k \right) = 0 \tag{1}$$

$$\begin{aligned} \frac{\partial \rho_k \alpha_k \vec{u}_k}{\partial t} + \nabla \cdot \left(\rho_k \alpha_k \vec{u}_k \vec{u}_k \right) &= -\alpha_k \nabla P + \alpha_k \rho_k \vec{g} \\ &+ \nabla \cdot \left[\alpha_k \mu_k^e \left(\nabla \vec{u}_k + \left(\nabla \vec{u}_k \right)^T \right) \right] + \vec{F}_k \end{aligned} \tag{2}$$

where F_k represents the sum of the interfacial forces that include the drag force F_D, lift force F_L, virtual mass force F_{VM}, wall lubrication force F_{WL} and turbulent dispersion force F_{TD}. Turbulence of the liquid phase is modelled using a standard k-ε model while a zero equation turbulence model is employed for the disperse phase. Bubble induced turbulence caused by wakes of bubbles is accounted according to Sato's bubble-induced turbulent viscosity [9].

Detail descriptions of the interfacial forces that appear in the momentum equation can be found in Anglart and Nylund [10]. Briefly, the inter-phase momentum transfer between gas and liquid due to drag force is given by

$$F_D = \frac{1}{8} C_D a_{if} \rho_l \left| \vec{u}_g - \vec{u}_l \right| \left(\vec{u}_g - \vec{u}_l \right) \tag{3}$$

In a vertical pipe flow, the non-drag forces that are the lift, virtual mass, wall lubrication and turbulent dispersion are forces that are directed perpendicular to the flow direction. Lift force in terms of the slip velocity and the curl of the liquid phase velocity can be described as

$$F_L = \alpha_g \rho_l C_L \left(\vec{u}_g - \vec{u}_l \right) \times \left(\nabla \times \vec{u}_l \right) \tag{4}$$

Wall lubrication force, which is in the normal direction away from the heated wall and decays with distance from the wall, is expressed by

$$F_{WL} - \frac{\alpha_g \rho_l \left(\vec{u}_g - \vec{u}_l \right)}{D_s} \max \left(0, C_{w1} + C_{w2} \frac{D_s}{y_w} \right) \vec{n} \tag{5}$$

Turbulence induced dispersion taken as a function of turbulent kinetic energy and gradient of the void fraction of the of liquid yields in the form of:

$$F_{TD} = -C_{TD} \rho_l k \nabla \alpha_l \tag{6}$$

The drag coefficient C_D in equation (3) has been correlated for several distinct Reynolds number regions for individual bubbles according to Ishii and Zuber [11]. The constant C_L has been correlated according to Tomiyama [12] – a relationship expressed as a function of the Eotvos number that allows positive and negative lift coefficients depending on the bubble size. The correlation also accounts the effects of bubble deformation and asymmetric wake of the bubble. By default, the virtual mass coefficient C_{VM} takes the value of 0.5 while the wall lubrication constants C_{w1} and C_{w2} are –0.01 and 0.05 respectively. The coefficient C_{TD} is adjusted to 0.5 in the current study.

By definition, the interfacial area concentration a_{if} for bubbly flows can be determined through the relationship:

$$a_{if} = \frac{6 \alpha_g}{D_s} \tag{7}$$

where D_s is the bubble Sauter mean diameter. From the drag and non-drag forces above, it is evident that the interfacial area concentration a_{if} as well as the bubble Sauter man diameter in equation (7) are essential parameters that link the interaction between the liquid and gas (bubbly) phases. In most two-phase flow studies, the common approach of prescribing constant bubble sizes through the mean bubble Sauter diameter is still prevalent. Such an approach does not allow dynamic representation of the changes in the interfacial structure; the two-fluid model remains deficient in predicting flow transition behaviour from bubbly to slug regimes. In order to resolve the problem, the average number density transport equation, which allows changes in the two-phase flow structure to be predicted mechanistically, is introduced and described below.

Average Bubble Number Density Equation

The average bubble number density transport equation can be expressed as

$$\frac{\partial n}{\partial t} + \nabla \cdot \left(\vec{u}_g n \right) = \phi_n^{CO} + \phi_n^{BK} \tag{8}$$

where n is the bubble number density and ϕ_n^{CO} and ϕ_n^{BK} are the bubble number density variations induced by coalescence and breakage. Assuming a single bubble size given by the bubble Sauter mean diameter, the bubble number density for bubbly flow can be defined as

$$n = \frac{\alpha_g}{\pi D_s^3 / 6} = \frac{1}{36\pi} \frac{a_{if}^3}{\alpha_g^2} \tag{9}$$

It is observed that by solving the transport equation for the bubble number density n, the changes to the interfacial structure is locally accommodated throughout the flow. The inclusion of the source and sink terms in equation (8) caused by the phenomenological mechanisms of coalescence and breakage allows the description of the temporal and spatial evolution of the geometrical structure of the gas phase.

The coalescence and breakage effects due to the interactions among bubbles and between bubbles and turbulent eddies have been the subject of much attention. As fas as isothermal bubbly flow is concerned, the coalescence of bubbles is caused by the random collisions driven by turbulence (*RC*) and wake entrainment (*WE*) while the mechanism responsible for bubble breakage is caused by the impact of turbulent eddies (*TI*). These three mechanisms of coalescence and breakage developed by Wu et al. [4] have the form $\phi_n^{CO} = \phi_n^{RC} + \phi_n^{WE}$ and $\phi_n^{BK} = \phi_n^{TI}$:

$$\phi_n^{RC} = -0.021 \frac{\alpha_g^2 \varepsilon^{1/3}}{D_s^{11/3} \alpha_{\max}^{1/3} \left(\alpha_{\max}^{1/3} - \alpha_g^{1/3} \right)} \left[1 - \exp \left(- \frac{3 \alpha_{\max}^{1/3} \alpha_g^{1/3}}{\alpha_{\max}^{1/3} - \alpha_g^{1/3}} \right) \right]$$

$$\phi_n^{WE} = -0.0073 U_r \frac{\alpha_g^2}{D_s^4} \tag{10}$$

$$\phi_n^{TI} = 0.0945 \frac{\alpha_g \varepsilon^{1/3}}{D_s^{11/3}} \left(1 - \frac{We_{cr}}{We} \right) \exp \left(- \frac{We_{cr}}{We} \right)$$

where $\alpha_{\max}$, U_r, We and We_{cr} are the maximum allowable void fraction (= 0.80), relative velocity between the gas and liquid phases, Weber number and critical Weber number (= 2.0), respectively. It is noted that the relative velocity U_r is approximated by the consideration of the terminal velocity of a single isolated bubble.

Nevertheless, some experimental observations [13,14] argued that the coalescence due to wake entrainment is only significant between pairs of large cap bubbles (slug flow regime) in fluid sufficiently viscous to maintain their wake laminar; whereas small spherical or ellipsoidal bubbles tend to repel each other. As far as bubbly flows are concerned, Hibiki and Ishii [5] and Yao and Morel [6], therefore, considered only the coalescence of the bubbles governed mainly by the random collisions driven by turbulence. These two models are rather similar as can be observed below in their derivations. However, Yao and Morel [6] introduced the interaction time of the bubbles to coalesce and break-up in addition to the free travelling time as considered in their model as well as in Hibiki and Ishii [5] model. These coalescence and breakage mechanisms developed by Hibiki and Ishii [8] have the form

$$\phi_n^{CO} = -0.03\frac{\alpha_g^2\varepsilon^{1/3}}{D_s^{11/3}\left(\alpha_{\max}-\alpha_g\right)}\exp\left(-1.29\frac{\rho_l^{1/2}\varepsilon^{1/3}D_s^{5/6}}{\sigma^{1/2}}\right)$$

$$\phi_n^{BK} = 0.03\frac{\alpha_g\left(1\text{-}\alpha_g\right)\varepsilon^{1/3}}{D_s^{11/3}\left(\alpha_{\max}-\alpha_g\right)}\exp\left(-1.37\frac{\sigma}{\rho_l\,\varepsilon^{2/3}D_s^{5/3}}\right) \tag{11}$$

while in Yao and Morel [6] model, they have been derived as

$$\phi_n^{CO} = -2.86\frac{\alpha_g^2\varepsilon^{1/3}}{D_s^{11/3}}\frac{\exp\left(-1.017\sqrt{\frac{We}{We_{cr}}}\right)}{\frac{\alpha_{\max}^{1/3}-\alpha_g^{1/3}}{\alpha_{\max}^{1/3}}+1.922\alpha_g\sqrt{\frac{We}{We_{cr}}}}$$

$$\phi_n^{BK} = 1.6\frac{\alpha_g\left(1\text{-}\alpha_g\right)\varepsilon^{1/3}}{D_s^{11/3}}\frac{\exp\left(-\frac{We}{We_{cr}}\right)}{1+0.42\left(1\text{-}\alpha_g\right)\sqrt{\frac{We}{We_{cr}}}} \tag{12}$$

The maximum allowable void fraction in Hibiki and Ishii [5] and Yao and Morel [6] models retains the value of 0.52, which corresponds to the transition between the finely dispersed bubbly flow and slug flow. The critical Weber number in Yao and Morel [6] model is set to a value of 1.24.

Experimental Details

The two-phase flow experiment has been performed at the Thermal-Hydraulics and Reactor Safety Laboratory in Prudue University. The test section was a round tube made of acrylic with an inner diameter (D) of 50.8 mm and a length (L) of 3061 mm. The temperature of the apparatus was kept at a constant temperature (20°C) within the deviation of ±0.2°C by a heat exchanger installed in a water reservoir. Local flow measurements using the double sensor and hotfilm anemometer probes were performed at three axial (height) locations of z/D = 6.0, 30.3 and 53.5 and 15 radial locations of r/R = 0 to 0.95. A range of superficial liquid velocities j_l and superficial gas velocities j_g have been performed, which covered mostly the bubbly flow region, including finely dispersed bubbly flow and bubbly-to-slug transition flow regions. Area averaged superficial gas velocity $\langle j_g \rangle$ was obtained from local void fraction and gas velocity measured by the double sensor probe, whereas area averaged superficial liquid velocity $\langle j_l \rangle$ was obtained from local void fraction measured by the double sensor probe and local liquid velocity measured by the hotfilm anemometry. More details regarding the experimental set-up can be found in Hibiki and Ishii [5]. In this paper, numerical predictions have been compared against local measurements at the flow conditions: $\langle j_l \rangle$ of 0.986 m/s, $\langle j_g \rangle$ of 0.0473 m/s, inlet void fraction of 5% and inlet bubble size of 3 mm.

Numerical Details

Solution to the two sets of governing equations for momentum was sought. Radial symmetry has been assumed, so that the numerical simulations could be performed on a 60° radial sector of the pipe with symmetry boundary conditions at both sides. Inlet conditions were assumed to be homogeneous in regards to the superficial liquid and gas velocities, void fractions for both phases and uniformly distributed bubble size in accordance with the flow conditions described above. At the pipe outlet, a relative average static pressure of zero was specified. A three-dimensional mesh containing hexagonal elements was generated resulting in a total of 30000 elements covering the entire pipe domain. Reliable convergence was achieved within 400 iterations for a satisfied convergence criterion based on the RMS (Root Mean Square) residuals of 1.0e-4 and for a physical time scale of the fully implicit solution method of 0.01 s.

Results and Discussion

The local radial profiles of the void fraction, interfacial area, bubble Sauter mean diameter, vapour and liquid velocities at two axial locations of z/D = 6.0 and 53.5 are predicted through the two-fluid and population balance models.

Figure 1 shows the void fraction distributions at the two axial locations for the measured data and results obtained from the various coalescence and breakage models employed in the average bubble number density transport equation. In isothermal gas-liquid bubbly flows, Serizawa and Kataoka [15] classified the phase distribution patterns into four basic types of distributions: "wall peak", "intermediate peak", "core peak" and "transition". The void fraction peaking near the pipe wall represented the flow phase distributions caused by the typical "wall peak" behaviour. From these results, it was observed that a well–developed wall peaking occurred further downstream at the axial location of z/D = 53.5 (near the exit) instead at the location of z/D = 6.0 (near the inlet). The three model predictions of the radial void fraction distributions could be seen to capture the similar behaviour trends with the measurements very well at these two locations.

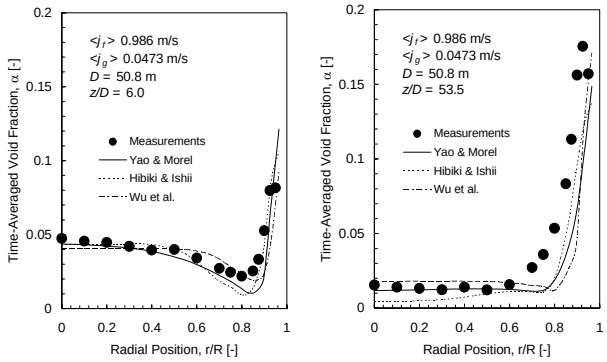

Figure 1. Local predicted and measured void fraction profiles at z/D = 6.0 and 53.5.

Figure 2 illustrates the interfacial area concentration distributions for the respective two axial locations for the measurements and the three model predictions. The measured data followed the similar profile as the void fraction distribution as stipulated in Figure 1. From these results, the three coalescence and breakage models compared very well with the experimental data. Nevertheless, the bubble Sauter mean diameter distribution in

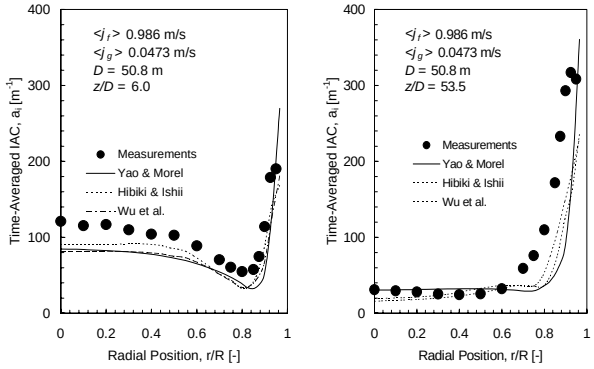

Figure 2. Local predicted and measured interfacial area concentration profiles at z/D = 6.0 and 53.5.

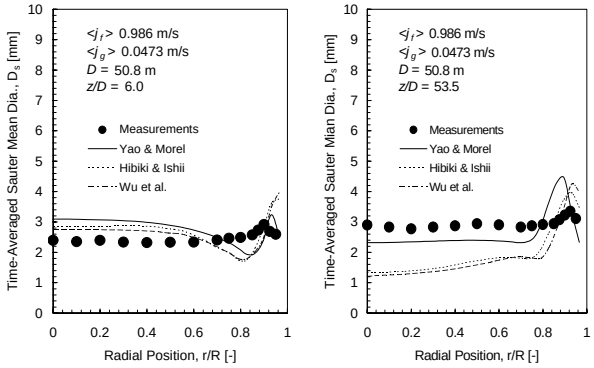

Figure 3. Local predicted and measured bubble Sauter mean diameter profiles at z/D = 6.0 and 53.5.

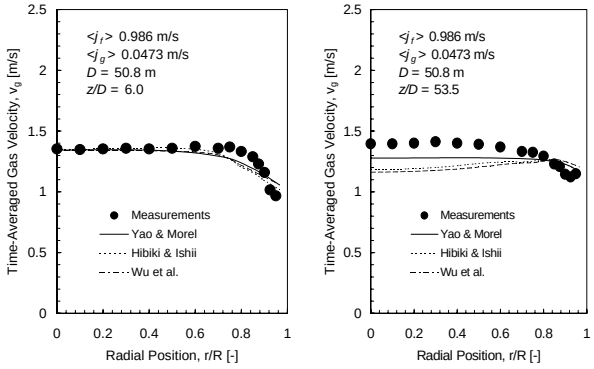

Figure 4. Local predicted and measured gas velocity profiles at z/D = 6.0 and 53.5.

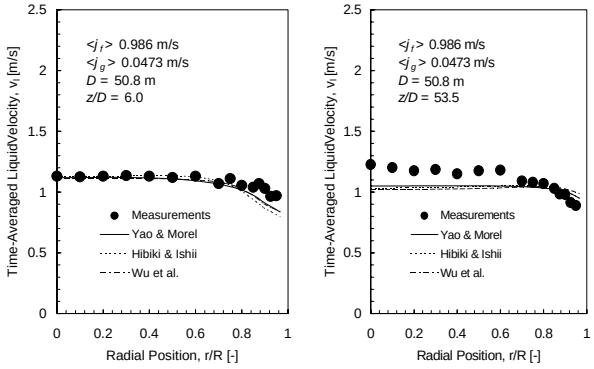

Figure 5. Local predicted and measured liquid velocity profiles at z/D = 6.0 and 53.5.

Figure 3 was better predicted by Yao and Morel [6] model at z/D = 53.5 in comparison to the model predictions made by Wu et al. [4] and Hibiki and Ishii [5].

Figures 4 and 5 show the local radial vapour and liquid velocity distribution at the two axial locations. The introduction of bubbles into the liquid flow had the tendency to flatten the liquid velocity profiles with a relatively steep decrease close to the pipe wall. The same behaviour was also observed for the gas velocity profiles. Overall, all the three model predictions of the gas and liquid velocities were in satisfactory agreement with measurements.

Conclusions

A two-fluid model coupled with population balance approach is presented in this paper to handle isothermal gas-liquid bubbly flows. The average bubble number density transport equation was formulated and implemented in the CFD code CFX5.7 to determine the temporal and spatial geometrical changes of the gas bubbles. Coalescence and breakage mechanisms by Wu et al. [4], Hibiki and Ishii [5] and Yao and Morel [6] were assessed against experiments performed at Prudue University. Satisfactory agreements were achieved for the void fraction, interfacial area concentration, bubble Sauter mean diameter and gas and liquid velocities against measurements.

References

[1] Delhaye, J.M. & Bricard, P., Interfacial Area in Bubbly Flow: Experimental Data and Correlations, *Nuc. Eng. Des.*, **151**, 1994, 65-77.

[2] Kocamustafaogullari, G., Huang, W.D. & Razi, J., Measurement of Modeling of Average Void Fraction, Bubble Size and Interfacial Area, *Nuc. Eng. Des.*, **148**, 1994, 437-453.

[3] Lehr, F. & Mewes, D., A Transport Equation for the Interfacial Area density Applied to Bubble Columns, *Chem. Eng. Sci.*, **56**, 2001, 1159-1166.

[4] Wu, Q., Kim, S., Ishii, M. & Beus, S.G., One-Group Interfacial Area Transport in Vertical Bubbly Flow, *Int. J. Heat Mass Transfer*, **41**, 1998, 1103-1112.

[5] Hibiki, T., & Ishii, M., Axial Interfacial Area Transport of Vertical Bubbly Flows, *Int. J. Heat Mass Transfer*, **44**, 2001, 1869-1888.

[6] Yao, W., & Morel, C., Volumetric Interfacial Area Prediction in Upwards Bubbly Two-Phase Flow, *Int. J. Heat Mass Transfer*, **47**, 2004, 307-328.

[7] Lo, S., Application of Population Balance to CFD Modelling of Bubbly Flow via the MUSIG model, AEA Technology, *AEAT-1096*, 1996.

[8] Yeoh, G.H. & Tu, J.Y., Population Balance Modelling for Bubbly Flows with Heat and Mass Transfer, *Chem. Eng. Sci.*, 2004, in press.

[9] Sato, Y., Sadatomi, M. & Sekoguchi, K., Momentum and Heat Transfer in Two-Phase Bubbly Flow-I, *Int. J. Multiphase Flow*, **7**, 1981, 167-178.

[10] Anglart, H. & Nylund, O., CFD Application to Prediction of Void Distribution in Two-Phase Bubbly Flows in Rod Bundles, *Nuc. Sci. Eng.*, **163,** 1996**,** 81-98.

[11] Ishii, M. & Zuber, N., Drag Coefficient and Relative Velocity in Bubbly, Droplet or Particulate Flows. *AIChE J.*, **25**, 1979, 843-855.

[12] Tomiyama, A., Struggle with Computational Bubble Dynamics, ICMF'98, 3rd Int. Conf. Multiphase Flow, Lyon, France, 1998, 1-18.

[13] Stewart, C.W., Bubble Interaction in Low-Viscosity Liquids, *Int. J. Multiphase Flow*, **41**, 1998, 1103-1112.

[14] Otake, T., Tone, S., Nakao, K. & Mitsuhashi, Y., Coalescence and Breakup of Bubbles in Liquids, *Chem. Eng. Sci.*, **32**, 1997, 377-383.

[15] Serizawa, I., & Kataoka, I., Phase Distribution in Two-Phase Flow, in N.H. Afgan (Ed.), *Transient Phenomena in Multiphase Flow*, Washington DC, 1988, 179-224.